ISSN 1392 - 1207. MECHANIKA. 2014 Volume 20(1): 35-41

Analysis of joining and division of gas bubbles based on measurements of their motion trajectories

M. R. Rzasa
Technical University of Opole, Mikolajczyka 5, 45-271 Opole, Poland, E-mail: m.rzasa@po.opole.pl

crossref http://dx.doi.org/10.5755/j01.mech.20.1.6596

1. Introduction

There are many papers on the gas bubble motion in the liquid [1-5], but the problem has not been completely recognized so far. The process of bubble formation and distribution of the forces influencing them is very complicated. Moreover, a numerical analysis of the bubble motion must include motion of the liquid carrying the bubbles, or its motion caused by the bubble motion. Because of complexity of those motions and the forming turbulences, experiments are often necessary if we want to evaluate the bubble behaviour.

The gas bubble motion is relatively complex and it strongly depends on distribution of forces acting to the moving bubble. Fig. 1 shows a basic system of forces acting to the bubble moving upward in a stationary liquid. Depending on the bubble size and shape, participation of particular forces varies. In a consequence, trajectories of motion of the bubbles moving in a liquid can be irregular, the bubbles often join or disintegrate.

Bubble velocity is influenced by four basic forces: the hydrostatic lift force (directed upward) F_w, the resisting force F_v and the inertial force F_b, oppositely directed to the motion direction, and the Magnus force F_M generating as a result of gas circulation inside the bubble and the liquid flowing around it. The resisting and inertial forces can be often distributed into two components: one conforming with the flow direction, and the other – transverse to the flow direction.

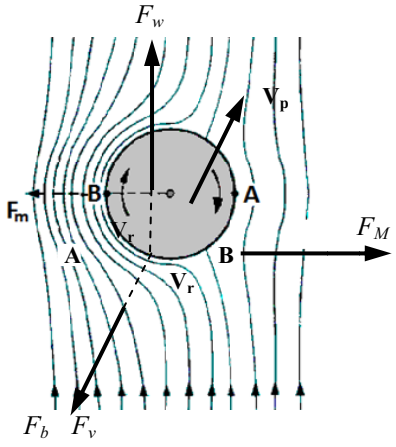

Fig. 1 General view of a specimen with side grooves

The hydrostatic force F_w is determined by the Archimedes' principle:

$$F_w = \left(\rho_c - \rho_g\right) g V_p , \tag{1}$$

where g acceleration of gravity, m/s^2, V_p volume of the bubble, m^3, ρ_g, density of the gas, kg/m^3, ρ_c density of the liquid, kg/m^3.

A general relationship for the resisting force F_v is written as:

$$F_v = C_D A_p \rho_c \frac{v_p \left| v_p \right|}{2}, \tag{2}$$

where C_D resistance coefficient, A_p area of the bubble section in the horizontal plane, m^2, v_p velocity of the bubble flow, m/s.

$$C_D = max\left[min\left[\frac{16}{Re}\left(1+0{,}15Re^{0{,}687}\right);\ \frac{48}{Re}\right];\ \frac{8}{3}\frac{Eo}{Eo+4}\right]; \tag{3}$$

$$C_D = max\left[min\left[\frac{24}{Re}\left(1+0{,}15Re^{0{,}687}\right);\ \frac{72}{Re}\right];\ \frac{8}{3}\frac{Eo}{Eo+4}\right]; \tag{4}$$

$$C_D = max\left[\frac{24}{Re}\left(1+0{,}15Re^{0{,}687}\right);\ \frac{8}{3}\frac{Eo}{Eo+4}\right], \tag{5}$$

where the Eötvösa Eo and Reynolds numbers Re were defined as:

$$Eo = \frac{g\left(\rho_c - \rho_g\right) d_p^2}{\sigma_c}; \tag{6}$$

$$Re = \frac{v_p d_p \rho_c}{\eta_c}, \tag{7}$$

where σ_c coefficient of surface tension of the liquid, N/m, d_p diameter of the bubble, N/m, η_c liquid viscosity, Pa·s.

Determination of the resistance coefficient C_D for the bubbles continuously changing their shapes is not easy; it is often impossible to define it precisely. Akio Tomiyama [6] proposed an expression for approximate determination of C_D, dependent on the liquid impurity. Eq. (3) concerns a pure liquid, Eq. (4) is for a little impure liquid. Eq. (5) is formulated for an impure liquid. The author thinks that Eq. (4) should be applied for municipal water because it should be understood as contaminated by mineral compounds. Eq. (3) can be applied only in the case of water which was distilled many times. This example illustrates complexity of the considered problem and difficulties in precise determination of the resistance coefficient because it is not possible to include all the factors influencing its value.

The moving bubble puts the surrounding liquid in

motion, in a consequence the inertial force is generated. The inertial force can be determined as a half of volume of the bubble of density of the surrounding liquid [7]. It can be written as:

$$F_b = \rho_c \frac{\pi d_p^3}{12} \frac{dv_p}{dt} . \tag{8}$$

The Magnus force generates the bubble motion in transverse direction. It is a result of pressure difference at the opposite ends of the bubble (points A and B). The Magnus force can be calculated according to the Bernoulli equation. Thus, the carrying force can be written as [7, 8]:

$$F_M = \rho_c \frac{\pi d_p^2}{4} v_p v_r , \tag{9}$$

where v_r rotational speed of the bubble, m/s.

The above equation includes rotational speed v_r connected with gas circulation inside the bubble. Such circulation is dependent on both dimensions and shapes of the bubbles. Precise determination of the speed is very difficult or even impossible. Thus, in the case of the bubble motion the Magnus force is determined from empirical relationships [6, 8].

From the above considerations it appears that theoretical determination of the bubble motion trajectory is often impossible. Thus, it is necessary to complete theoretical considerations with the experimental results. The paper presents a measuring method and the measurement results for the air bubbles moving in a motionless water.

2. The test stand

Structure of the test stand is shown in Fig. 2. The basic element is a vertical column *1* (0.2 × 0.2 × 1.5 m), containing water.

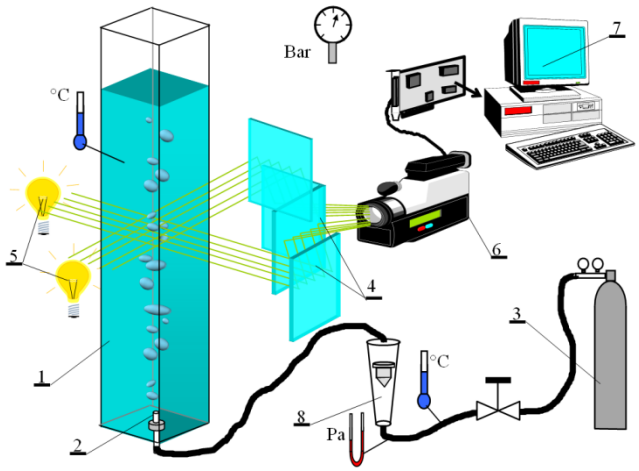

Fig. 2 The test stand

On the base there is an exchangeable jet *2*. Air is delivered by the jet from the gas cylinder *3*, and the air flow is measured with the flowmeter *8*. In the central part of the column there is a system of mirrors *4*. Two halogen lights *5* of 1500 W are the light sources. The image is registered by a digital camera *6* with a triple converter CCD made by CANON CANON MX1. The image from the camera is sent to the computer *7* by the interface IEEE 1394. Measurements were realized under the controlled external conditions.

The system of mirrors contains four mirrors located at the angle 2 × 45°, 2 × 22.5°. It allows to obtain images of the column from two sides of exposure synchronized at time. Such solution allows to register an image with only one camera, so difficult synchronization of images is not required and reconstruction becomes easier.

An image from the camera is used for determination of a spatial velocity distribution. The successive frames allow to determine a sense and a value of the vector of the moving bubble velocity, thus determination of the motion trajectory is possible. Volume and surface are calculated by approximation of the bubble shapes by known geometrical figures.

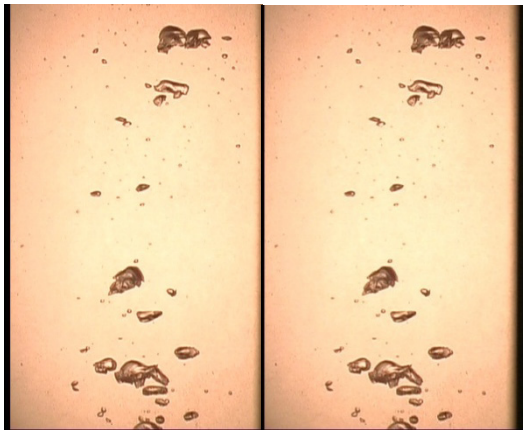

a

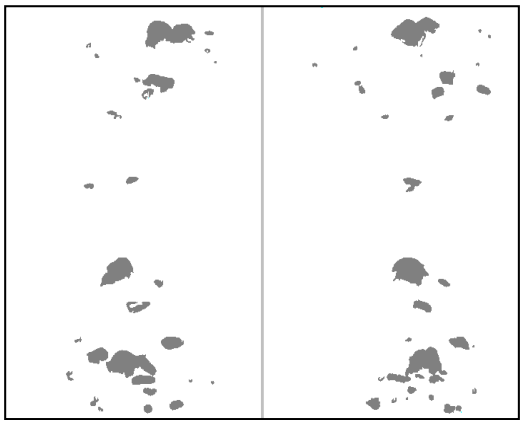

b

Fig. 3 Bubble flows a) from a video camera; b) after binearization

Fig. 3, a shows a typical flow image registered with a camera of the image tomograph. Velocities of particular bubbles are strongly different. The bubbles often join or divide during the flow and reconstruction becomes difficult. The algorithm of reconstruction includes some stages. At the first stage the objects are separated from the image and segregated, and next their positions are determined according to the successive frames of the image. It is done in the image converted into a binary form (Fig. 3, b) [9].

A shape of a moving bubble was continuously varying at time, so the center of mass was assumed as the reference point for determination of the bubble path. From

the tomograph we obtain two images of the bubble seen from two sides, so the center of mass is determined for each image separately (Fig. 4). Determination of coordinates x_c and y_c of the center of mass is realized according to the following relationship.

$$x_c = \frac{\sum A_p x_i}{\sum A_p}; \qquad y_c = \frac{\sum A_p y_i}{\sum A_p}, \tag{10}$$

where: A_p area of one pixel of the image, x_i, y_i coordinates of the i-th pixel.

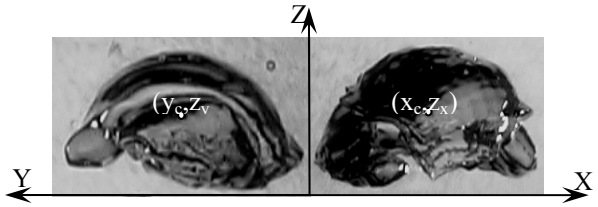

Fig. 4 Idea of determination of the bubble center of mass

Centres of mass along the axis Z for two bubble images can be a little different. Thus, the averaged value was assumed for z_x and z_y z_x and z_y.

$$z = \frac{z_x + z_y}{2}. \tag{11}$$

Velocity of the moving bubble can be determined from the shift vector in the successive frames of the image at the known time resulting from a number of frames per second. The velocity is expressed as:

$$v_g = \frac{\sqrt{\left(x_n + x_{n-1}\right)^2 + \left(y_n + y_{n-1}\right)^2 + \left(z_n + z_{n-1}\right)^2}}{t_k}, \tag{12}$$

where: x_n, y_n, z_n coordinates of the centre of mass for the n-th frame of the image, x_{n-1}, y_{n-1}, z_{n-1} coordinates of the centre of mass for the n-1 frame, t_k time between the successive frames.

The bubble shapes were approximated by ellipsoid. It is realized during reconstruction based on determination of ellipsoid diameters and points of contact (A, B, C) of ellipsoid with sides of the prism circumscribed on the ellipsoid (Fig. 5) [10].

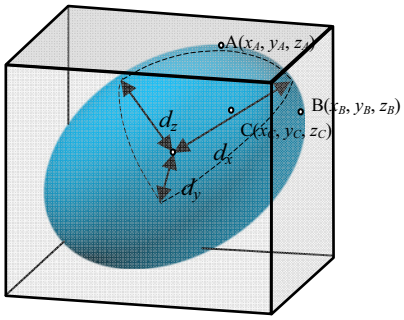

Fig. 5 Idea of approximation of the bubble shape

3. The test results

Tests of the gas bubble flow in the aeration column were performed for various gas streams flowing from the nozzle 2 mm in diameter.

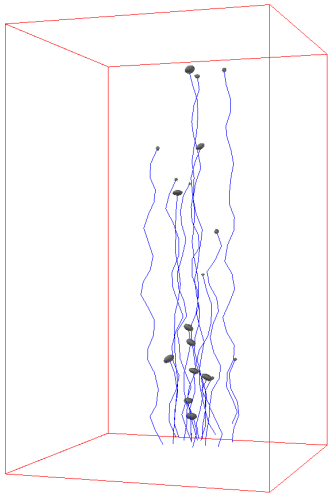

Fig. 6 Reconstruction of the bubble motion trajectories for gas streams 0.27 cm^3/s

In the case of very small gas streams (Fig. 6) bubble motion performs along a screw line, it causes a continuous change of shapes and spatial positions of the bubbles. From the above results it appears that even very small bubbles not always remain spherical. Volumes of the moving bubbles are similar, however greater bubbles move much closer to the gas core and they strongly influence the liquid circulation. The liquid circulation influences motion of the bubbles moving near the core. Trajectories of the bubbles inside the gas core are more similar to the straight line than those occurring far from the gas core. In the case of small gas streams joining or disintegration of the bubbles cannot be observed. Differences in volume of the bubbles can be seen only during their formation.

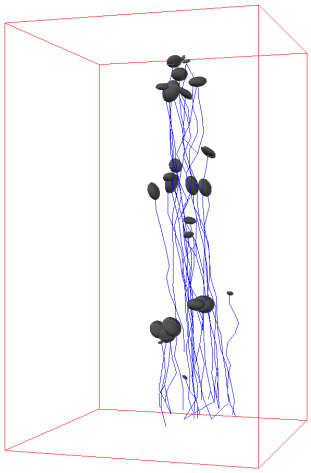

Fig. 7 Reconstruction of the bubble motion trajectories for gas streams 5.5 cm^3/s

In the case of greater gas streams (Fig. 7), velocity of the moving bubbles and their number in the gas core strongly increase. Moreover, joining of the bubbles can be a result of their collision. Like in the case of small streams, there are single bubbles, trajectory of which is a little distant from the gas core. It is a result of a more intense circulation of the liquid caused by the bubble motion and in a consequence the bubbles get into the gas core. Thus, a

number of small bubbles moving far from the gas core is much smaller. Turbulences in the gas core cause that diameter of the core begins to pulse, and in a consequence the core becomes conical. A high number of bubbles of very small volumes is present near very big bubbles. The small bubbles outside the gas core behave similarly like those in the case of lower flow rates. Resistances of motion cause large deformation of the shape even when the trajectory remains screw.

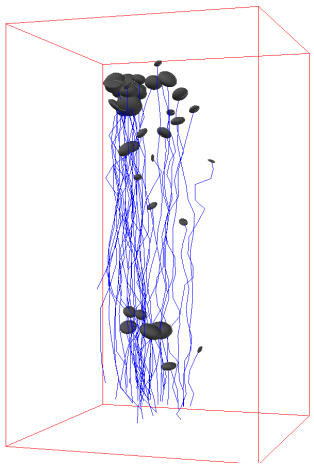

Fig. 8 Reconstruction of the bubble motion trajectories for gas streams 11 cm^3/s

In the case of greater gas streams turbulences in the gas core increase significantly (Fig. 8). Then, the gas core becomes to oscillate around the vertical axis of the column. Let us notice that greater bubbles move as a group, and smaller bubbles separate from the circulating group and move along independent paths up to the moment when they got to the circulating core again. Numerous bubbles join together, or form greater agglomerates and move as a group of mixing bubbles. Big bubbles often divide into some smaller ones. There are many interactions between the moving bubbles because of a great number of bubble and higher velocities of motion of the bubbles moving in the neighbourhood. Strong mutual interaction between the bubbles can be observed, so their motion is disturbed, in practice there is no free motion of the bubbles. Increase of the gas stream causes increase of intensity of gas core circulation and, in a consequence, increase of its diameter.

In the case of big gas streams we can notice groups of bubbles (Fig. 9). In such groups, the bubbles always join or divide. Shapes of such bubbles are irregular and they are subjected to fast deformations. In a group of big bubbles we can often notice the moving small bubbles of diameter similar to a ball. They form as a result of disintegration of greater bubbles. Let us notice occurrence of a great number of small bubbles both inside and outside of the gas core centre. Greater bubbles move in groups so the flow becomes pulsating. The flow is very turbulent, the bubbles move very fast, so their joining and divisions are intense. Influence of big bubbles is so strong that smaller bubbles in their neighbourhood move along the trajectories similar to the trajectory of the moving big bubble. Downward motion of short duration can be also observed – it concerns small bubbles. Such phenomenon can be usually seen when a very small bubble forms as a result of disintegration of a big bubble. Turbulences of a liquid generated as a result of such division cause that a motion direction of a small bubble changes, and forces connected with turbulence of the liquid are relatively high, and the bubble begins to move in the opposite direction to the force of the hydrostatic lift.

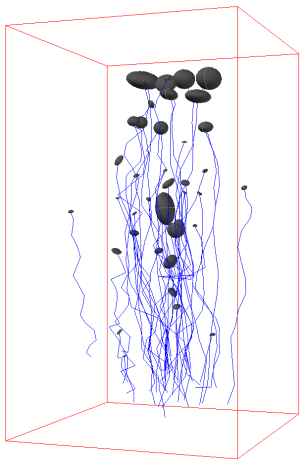

Fig. 9 Reconstruction of the bubble motion trajectories for gas streams 39 cm^3/s

3.1. Tests of the bubble motion trajectories

The author tested how a shape of the bubble motion trajectories changes for different dimensions. Przeprowadzono badania jak zmienia się kształt trajektorii ruchu pęcherzyków of the bubbles. Fig. 10 presents the results obtained for the bubbles moving in a stationary liquid. The images of each bubble were presented in two views: end view and from above of its motion axis. The bubbles of small diameters (from 3 to 10 mm) move along a screw line. Since all the turbulences of the liquid strongly influence the motion, the trajectories are not always regular screw lines. As the bubble diameter increases, velocity of the bubble increases, and the radius of its motion trajectory curvature decreases. The bubbles of diameters from 10 to 20 mm are characterized by a small screw motion with distinct oscillations of the bubbles. Their shape is similar to a flattened ellipsoid. Circulations around the axis cause increase of the motion resistances, and velocity of the bubbles decreases. Observing the bubble views from above we can see that curvature of the screw line is similar to the bubble diameter. Big bubbles of diameters more than 20 mm do not move along the screw line but they move along the zig-zag line, however they still oscillate around their axes.

Motion of small bubbles is strongly influenced by circulation of the liquid. For small bubble diameters (4 to 7 mm), when they move far from the gas core they behave similarly like in the stationary liquid. Their trajectories have screw shapes. As they are more close to the gas core centre, their velocities increase and the radius of trajectory curvature decreases. As the gas stream from the jet increases, trajectory of small bubbles becomes more rectilinear. It means that the bubble motion is determined by the liquid motion in the gas core.

The bubbles of diameters 15 to 20 mm are less dependent on changes of the motion trajectory depending on a distance from the gas core. Only the motion velocity caused by the liquid motion changes.

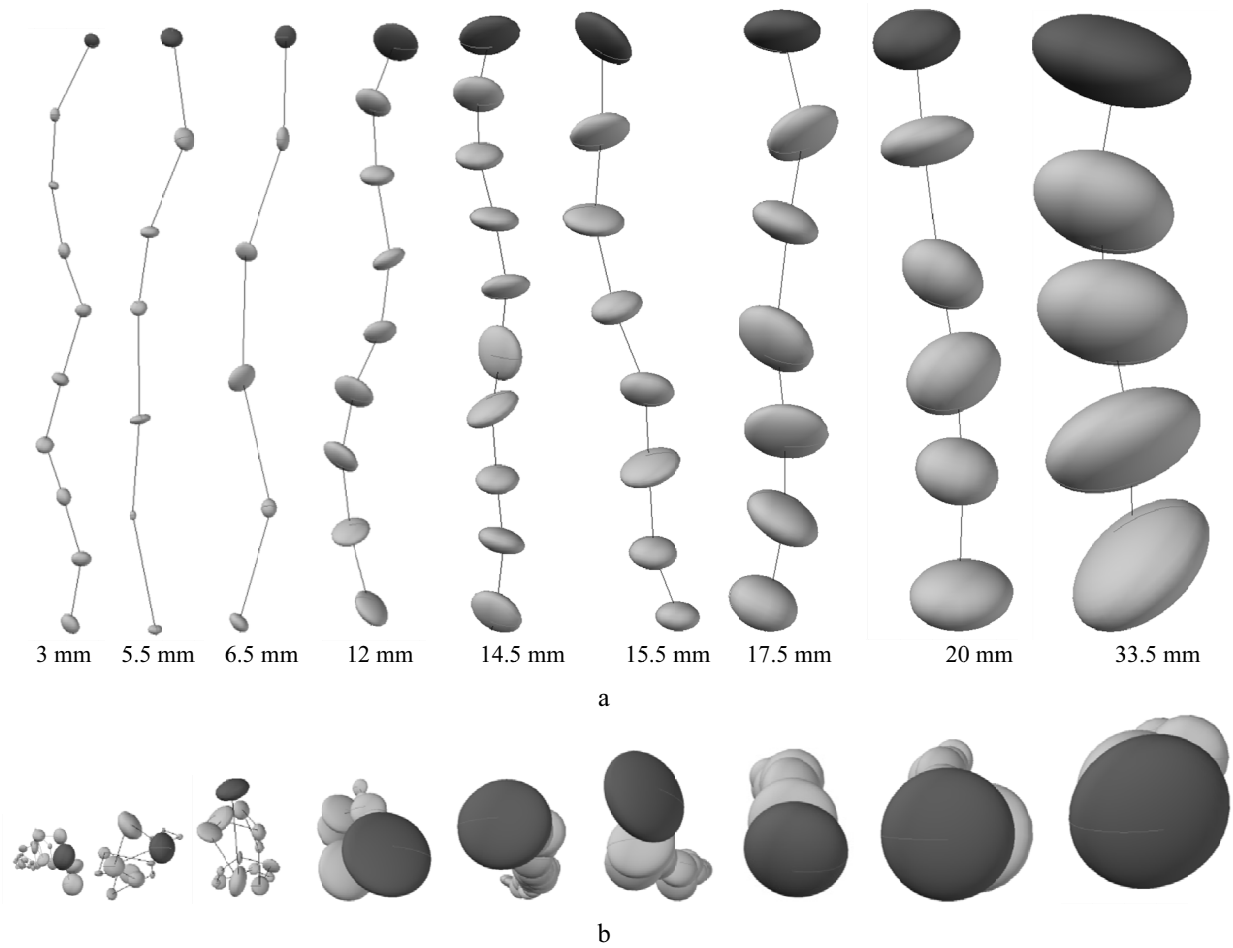

Fig. 10 Trajectories of motion of the bubbles moving in water depending on their dimensions a) end view; b) top view

3.2. Tests of interactions between the moving bubbles

Interactions between the bubbles strongly influence their motion and the moving direction. The interaction can cause changes of the motion trajectory resulting from the liquid swirl caused by motion of the other bubbles, or can lead to their joining or division. For gas streams less than 2.5 cm^3/s, joining or disintegration of the bubbles is not observed, we can notice only mutual disturbances of motion caused by the liquid swirl. As the gas stream increases, disintegration becomes more intense.

Independently on the gas stream, disintegration of the bubbles is usually caused by joining of two bubbles of similar dimensions moving in the neighbourhood with similar velocities. As volume of the bubble increases, we obtain higher resistances of motion and turbulences caused by motion of the big bubble, greater forces acting to the bubble cause division of the bubble into some smaller ones. This process is shown in Fig. 11. It contains some stages: at first, the bubble is divided into two parts, and after some time the two parts are divided into more parts. The forming bubbles are often smaller than the primary bubble. It is a result of big turbulences of the liquid while dividing near the bubble, the Magnus force is generated and its direction changes very fast. Such unstationary and greater distribution causes division of the bubble.

Disintegration can be also caused by collision of one big and one small bubble, where the small bubble moves much quickly (Fig. 12). Since a volume of the small bubble is much more smaller, it cannot cause such big increase of the bubble volume resulting in division previously described. In such a case, disintegration is caused by disturbance of air circulation inside the bubble. Air motion in big bubbles causes reduction of the Magnus force, so big bubbles in free motion move with much less oscillations than small bubbles. However, disturbance of circulation

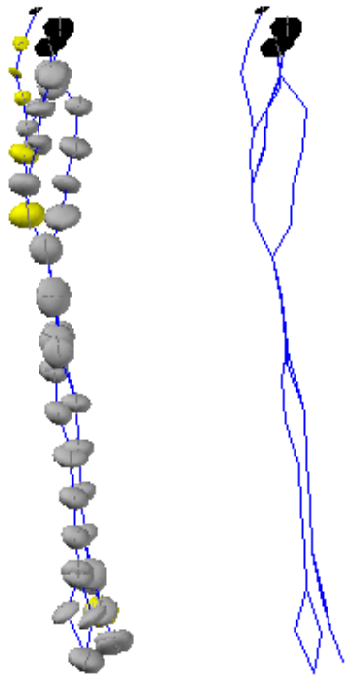

Fig. 11 Disintegration of the bubbles as a result of joining of two bubbles

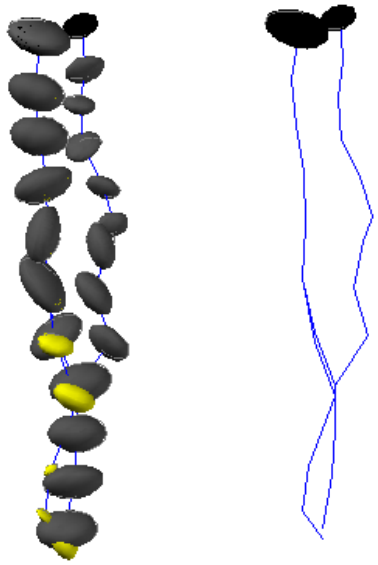

Fig. 12 Disintegration of the bubbles as a result of collision of the big bubble with the small one

causes increase of the side force resulting in deformation. It causes increase of the force of resistance and – in a consequence – the bubble disintegration.

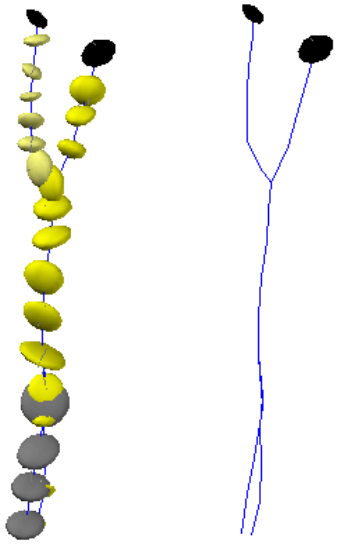

Fig. 13 Bubble disintegration caused by increase of motion velocity for gas stream 8.3 cm^3/s

The bubble disintegration can be also caused by increase of the bubble motion velocity resulting from increase of the force of hydrostatic lift caused by increase of the bubble volume (Fig. 13). This process begins with collision of the big and small bubbles. Velocity of the small bubble is relatively low, and it does not cause such a big change of air circulation inside the bubble, so disintegration does not take place. However, increase of the bubble volume caused by joining with the smaller bubble cannot be neglected and velocity of the bubble motion begins to increase. In a consequence, the force of resistance increases and causes the bubble flattening and next its disintegration. Let us notice that the disintegrating bubbles are influenced by transverse forces causing that the distance between new bubbles becomes greater. From many observations it appears that transverse forces are proportional to volume of the moving bubble.

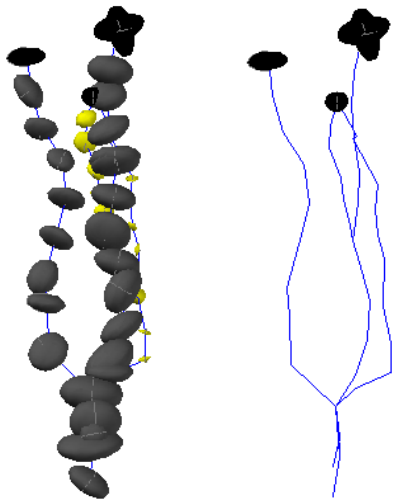

Fig. 14 Bubble disintegration caused by increase of motion velocity for gas stream 39 cm^3/s

In the case of big gas streams we can observe formation of very big bubbles (Fig. 14). Increase of the bubble velocity causes disintegration of the bubble from the same reasons as those presented in Fig. 8, a. However in this case the transverse forces occurring while disintegrating are big and the bubble divides into some smaller ones, usually two similar bubbles and the third one is much smaller.

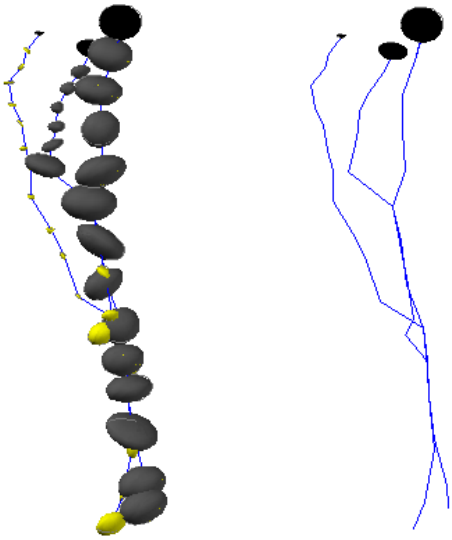

Fig. 15 Bubble disintegration caused by increase of motion velocity for gas stream 8.3 cm^3/s

The small bubble forming as a result of disintegration of the big bubble changes its motion direction very quickly and becomes more distant from the gas core. Big acceleration can be observed during the first phase of that process (Fig. 15). The forming small bubbles often cause further divisions in a consequence of collisions with other big bubbles.

The described phenomena causing bubble disintegration are usually continuous, and many of them proceed at the same time. Thus, continuous mixing of the moving bubbles (Fig. 16). Depending on the gas stream, the area occupied but such a group of bubbles enlarges. Determination of the dominating reason of the bubble disintegration is difficult.

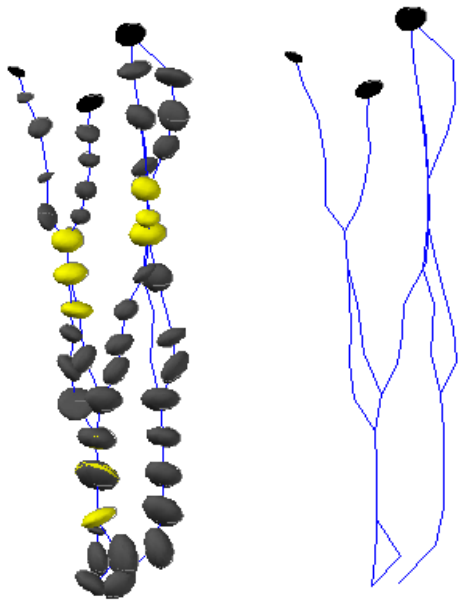

Fig. 16 Continuous disintegration and joining of bubbles for gas stream 11 cm^3/s

4. Conclusion

Typical behaviours of gas bubbles moving in water were considered. It appears that the motion character is complex, and many interactions can be seen. Such situation is influenced by many factors, it is often not possible to determine them in theoretical considerations. Works on determination of typical mechanisms of gas bubble disintegration should be helpful in elaboration of theoretical models describing motion and interactions between the moving bubbles. This problem is important from the point of view of mass exchange and determination of aeration intensity in many fields of chemical industry, sewage treatment or extractive industry.

References

1. **Kolev, N.I.** 2007. Multiphase Flow Dynamics, Fundamentals, Springer, 758 p. http://dx.doi.org/10.1007/3-540-69833-7.
2. **Kolev, N.I.** 2012. Multiphase Flow Dynamics, Mechanical Interaction, Springer, 366p.
3. **Brennen, C.E.** 2005. Fundamentals of Multiphase Flows, Cambridge University Press, 410 p.
4. **Dziubiński, M.; Prywer, J.** 2010. Mechanika płynów dwufazowych; WNT, Warszawa.
5. **Kowalczyk, A.; Hanus, R.; Szlachta, A.** 2011. Investigation of the statistical method of time delay estimation based on conditional averaging of delayed signal, Metrology and Measurement Systems 18(2): 335-342. http://dx.doi.org/10.2478/v10178-011-0015-3.
6. **Tomiyama, A.** 1998. Struggle with computational bubble dynamics, Third International Conference on Multiphase Flow, ICMF`98, Lyon France, 1-18 p.
7. **Mikielewicz, D.** 2002. Modelowanie wymiaru pędu I ciepła w dwufazowym przepływie pęcherzykowym, Monografia Politechnika Gdańska.
8. **Tomiyama, A.; Sou, A.; Zun, I.; Kanami, N.; Sakaguchi, T.** 1995. Effects of Eötvös number and dimensionless liquid volumetric flux on lateral motion of a bubble in laminar duct flow, Advances in Multiphase Flow, Elsevier, 3-15 p.
9. **Chałubiec, J.; Rząsa, M.R.; Dobrowolski, B.** 2008. Application of image tomography for determination of gas flow parameters in aeration proces, 5th Internation Sympodium on Process Tomography in Poland, 25-26 August Zakopane.
10. **Rząsa, M.R.** 2011. Zastosowanie tomografii obrazowej do pomiaru parametrów poruszających się pęcherzyków gazu - algorytm rekonstrukcji, Przegląd Elektrotechniczny 87(9a): 116-120.

M. R. Rzasa

DUJŲ BURBULŲ SUSIJUNGIMO IR ATSISKYRIMO ANALIZĖ MATUOJANT JŲ JUDĖJIMO TRAJEKTORIJAS

R e z i u m ė

Darbe tiriamas oro burbulų grupės judėjimas atkreipiant dėmesį į jų tarpusavio sąveiką. Aprašoma testavimo stendo struktūra ir vaizdo tomografo idėja, kuria grindžiami burbulų judėjimo trajektorijos matavimai. Matavimų rezultatai pateikti trimatėje erdvėje analizuojant judančių burbulų tarpusavio sąveiką. Suklasifikuoti dujų burbulų atsiskyrimo mechanizmai.

M. R. Rzasa

ANALYSIS OF JOINING AND DIVISION OF GAS BUBBLES BASED ON MEASUREMENTS OF THEIR MOTION TRAJECTORIES

S u m m a r y

The paper presents considerations on motion of a group of air bubbles. Special attention has been paid to interactions between them. The author presents the test stand structure and the idea of image tomograph used for measurements of bubble motion trajectories. The results of measurements have been presented in a three-dimensional space, and next characteristic behaviours of the moving bubbles were analyzed. Some basic mechanisms of the gas bubble division have been classified.

Keywords: bubble interaction, two-phase flow measurement, imaging tomography.

Received March 19, 2013
Accepted February 11, 2014